value of λ. The extreme radial separations between the two curves (A4) lie on the line $R_\rho = \pm R_{\rho'}$ and thus the requirement that (A1) should be smaller than (A2) becomes

$$\frac{x^2-\alpha^2\lambda^2}{x-2b\alpha\lambda} > x \quad \text{or} \quad \frac{b}{\alpha} > \frac{\lambda}{2x}.$$

This is fulfilled for any value of λ if $b > \frac{1}{2}\alpha$, and for $\alpha = 1$ this leads to $|\cos(\mathbf{R}_\rho, \mathbf{R}_{\rho'})| > \frac{1}{2}$. Already this rough estimation yields a relatively wide angle between $\mathbf{R}_\rho$ and $\mathbf{R}_{\rho'}$ for which our assumption (A1)<(A2) is justified. Taking into account the $\mathbf{R}_\rho$ and $\mathbf{R}_{\rho'}$ dependence in a and considering values of λ which are smaller than λ_c, the allowed angle between R_ρ and $R_{\rho'}$ becomes even larger. Because the current-current correlation function (31) is itself proportional to b^2 the main contribution to it will arise from rather large values of b and in this region our assumption is justified.

PHYSICAL REVIEW VOLUME 140, NUMBER 6A 13 DECEMBER 1965

Low-Field de Haas–van Alphen Effect in Gold

A. S. JOSEPH, A. C. THORSEN, AND F. A. BLUM*
North American Aviation Science Center, Thousand Oaks, California
(Received 30 July 1965)

Detailed studies of the de Haas–van Alphen (dHvA) effect in Au single crystals have been carried out with a high-sensitivity torque magnetometer in steady fields up to 40 kG. The angular variations of all of the pertinent dHVA frequencies were determined to better than 0.1%. New low-frequency oscillations have been observed which appear to be associated with a difference frequency resulting from two extremal cross sections on the nearly spherical portion of the Fermi surface. Evidence has been obtained which suggests that the electron g factor for the neck orbits in Au may differ appreciably from the value 2.

I. INTRODUCTION

IT has been shown[1] that the Fermi surface in Au, like those in Cu and Ag, can be approximated by a distorted sphere which is multiply connected by necks along the ⟨111⟩ axes. In a recent paper[2] we have reported on a detailed study of the de Haas–van Alphen (dHvA) in effect in Ag, which provided evidence for the existence of two extremal cross sections around the nearly spherical portion, or "belly," of the Fermi surface. In order to examine more closely the fine details of the Fermi surface in Au, we have extended these measurements to several high-purity gold single crystals. As in the case of Ag, we have been able to measure accurately the changes of belly, dog's bone, rosette, and neck oscillations as functions of angle in the {100} and {110} planes. In contrast to the results on Ag, no evidence was found for the existence of two extremal belly orbits in Au when the magnetic field is near the ⟨111⟩ axis. We do, however, find that near the ⟨100⟩ axis there exist low-frequency oscillations similar to those observed in Ag. These may be attributed to the existence of two extremal cross sections of the nearly spherical portion of the Fermi surface.

II. EXPERIMENTAL

The experimental details of the null-deflection torsion balance have been described fully in previous reports.[2,3] The technique was similar to that used in Ag: changes in phase (defined as the ratio F/H_0, where F is the de Haas–van Alphen frequency and H_0 is the applied field) were monitored in a constant magnetic field as the field was rotated about the axis of suspension of the sample. This leads to a very accurate determination of the relative change in frequency, since each change in phase of the belly, for example, corresponds to a change in frequency of $\sim 0.001\%$. The dominant error in this type of measurement is in the determination of the angle at which the phase is measured. Typically this error can amount to $\approx 0.05°$. This leads to a relative accuracy in frequency of $\approx 0.01\%$ near a symmetry axis where the phase is not changing rapidly with angle. At angles away from symmetry directions where the phase changes rapidly with angle, the relative accuracy is reduced to $\approx 0.05\%$. It is estimated that the absolute accuracy of the frequency values is $\pm 0.6\%$.

The gold crystal used in the present study was grown in this laboratory by J. Savage and R. Guard, who used the Bridgman technique and a boron nitride crucible. The samples obtained from this crystal exhibited dHvA oscillations much stronger than those prepared in graphite crucibles and showed no experimental evidence

* Permanent address: Physics Department, California Institute of Technology, Pasadena, California.

[1] D. Shoenberg, Phil. Trans. Roy. Soc. (London) **A255**, 85 (1962).

[2] A. S. Joseph and A. C. Thorsen, Phys. Rev. **138**, A1159 (1965).

[3] A. S. Joseph and A. C. Thorsen, Phys. Rev. **133**, A1546 (1964), and references therein.

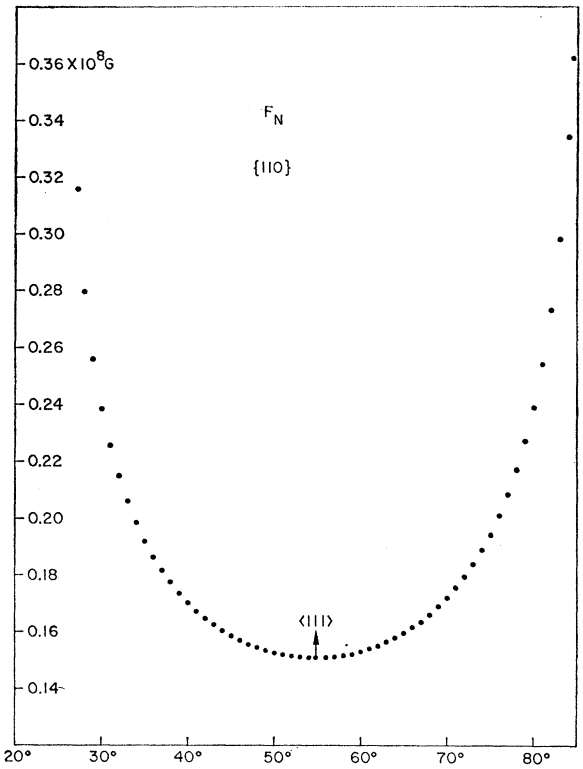

FIG. 1. Plot of the de Haas-van Alphen (dHvA) frequencies of the oscillations associated with the neck in the {110} plane as a function of the angle θ between the field and the ⟨100⟩ axis.

for small-angle dislocation boundaries. Two cylindrical samples were spark cut from the crystal along the ⟨110⟩ axis and one sample was cut along the ⟨100⟩ axis. The orienting and mounting procedures ensured that the magnetic field was oriented in the appropriate symmetry plane of the crystal to within 1°.

III. RESULTS AND DISCUSSION

The angular variations of the neck (F_N), belly (F_B), dog's bone (F_D), and four-cornered rosette (F_R) frequencies are shown in Figs. 1–4, 6, 7, and are tabulated in Tables I–V. In all cases the angle θ is measured from the ⟨100⟩ axis in the {110} plane and φ is measured from the ⟨100⟩ axis in the {100} plane. The absolute values for the various frequencies along the symmetry directions agree within experimental errors with those reported in Ref. 1. Effective masses of the neck, belly, and dog's bone are given in Table VI.

The neck oscillations are observed over an angular region wider than that reported earlier[4] because of the higher purity sample used in this experiment. The frequencies listed in Table I can be represented to better than 1% (except for the region $\theta \lesssim 32°$) by the

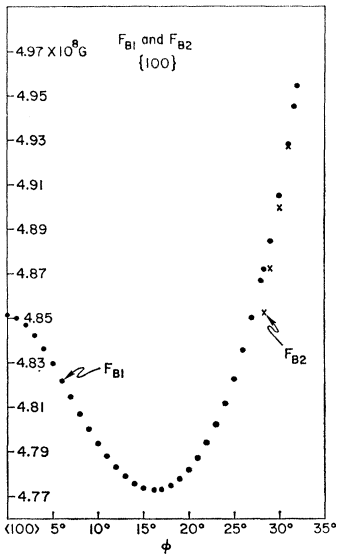

FIG. 2. Plots of the dHvA frequencies of the belly oscillations F_{B1} and F_{B2} in the {100} plane as functions of the angle φ between the field and the ⟨100⟩ axis. The values of F_{B2} are calculated according to $F_{B2}=F_{B1}-F_c$.

equation[5]

$$F(111)/F(\theta-54.75°) = \cos(\theta-54.75°)[1-(m_t/m_l)\tan^2(\theta-54.75°)]^{1/2},$$

with $m_t/m_l=2.35\pm0.05$. From the measured values of effective masses given in Table VI, we find $m_t=m^*(111)=0.29m_0$ and hence $m_l=0.124m_0$, where m_0 is the free electron mass. At $\theta=29.9°$ and $\theta=79.6°$, it was found that the amplitude of the oscillations nearly vanished, in a manner similar to the behavior in Cu[5] and Ag[2]. In these two metals this vanishing was attributed to the zero value of the spin-splitting factor $\cos[\pi g m^*/2m_0]$ in the theoretical expression for the amplitude of the torque.[6] Effective-mass measurements in Cu and Ag

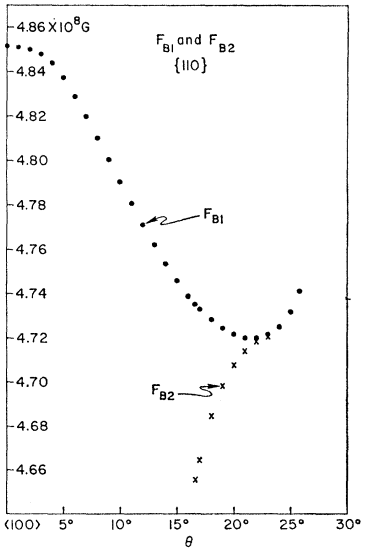

FIG. 3. Plots of the dHvA frequencies of the belly oscillations F_{B1} and F_{B2} in the {110} plane near the ⟨100⟩ axis as functions of θ. The values of F_{B2} are calculated according to $F_{B2}=F_{B1}-F_c$.

[4] A. S. Joseph and A. C. Thorsen, Phys. Rev. Letters **13**, 9 (1964).

[5] A. S. Joseph and A. C. Thorsen, Phys. Rev. **134**, A979 (1964).
[6] M. Cohen and E. I. Blount, Phil. Mag. **5**, 115 (1960).

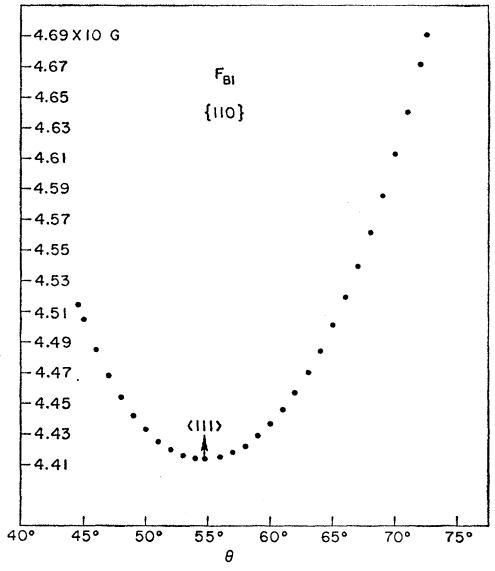

FIG. 4. Plot of the dHvA frequencies of the belly oscillations F_{B1} near the ⟨111⟩ axis in the {110} plane as a function of θ.

showed that the amplitude approached zero when m^*/m_0 assumed a value of 0.5 which leads to a zero value of this cosine term if the spectroscopic splitting factor $g=2$. In Au the amplitude approached zero at an angle where $m^*/m_0 \approx 0.59 \pm 0.02$ (see Table VI), approximately 1.2° from the angle where $m^*/m_0=0.5$. In order for the cosine term to explain the amplitude behavior, the g factor must be equal to $(2n+1)/0.59$, where $n=0, 1, 2, \cdots$, leading to the smallest values of 1.70 ± 0.06, 5.1 ± 0.2, etc. This is a considerable change from a value of 2 and differs from the findings for Cu and Ag. One might suspect that the effective-mass measurements may be affected by the presence of second harmonics since they would have their maximum amplitude in this angular region. However, the second harmonics present were not proportionately as strong as in Cu and Ag. Also, mass measurements taken near 4.2°K, where harmonics are relatively weak in amplitude, gave results identical with those made at lower temperatures. Measured values for m^* were typically reproducible between samples and at different fields and temperatures. Another possible explanation for the fact that the amplitude minimum does not occur where $m^*/m_0=0.5$ may involve a term in the theoretical ex-

TABLE I. F_N (in units of 10^8 G) in the {110} plane. The angle θ is measured from the ⟨001⟩ axis.

θ	F_N	θ	F_N	θ	F_N
27.1	0.3157	47	0.1555	66	0.1615
28	0.2795	48	0.1544	67	0.1636
29	0.2559	49	0.1534	68	0.1661
30	0.2385	50	0.1525	69	0.1689
31	0.2256	51	0.1519	70	0.1719
32	0.2149	52	0.1514	71	0.1754
33	0.2061	53	0.1510	72	0.1794
34	0.1984	54	0.1508	73	0.1838
35	0.1918	54.75	0.1508	74	0.1888
36	0.1863	55	0.1508	75	0.1944
37	0.1815	56	0.1510	76	0.2009
38	0.1773	57	0.1513	77	0.2084
39	0.1736	58	0.1518	78	0.2171
40	0.1702	59	0.1524	79	0.2269
41	0.1673	60	0.1531	80	0.2389
42	0.1647	61	0.1540	81	0.2541
43	0.1624	62	0.1551	82	0.2733
44	0.1603	63	0.1564	83	0.2976
45	0.1585	64	0.1579	84	0.3341
46	0.1569	65	0.1596	84.5	0.3622

TABLE II. F_{B1}, F_{B2}, F_C, F_R, and F_D (in units of 10^8 G) in the {100} plane. The angle φ is measured from the ⟨001⟩ axis.

φ	F_{B1}	F_R	φ	F_{B1}	F_{B2}	F_C	φ	F_D
0	4.8513	2.0074	18	4.7747			35	···
1	4.8499	2.0089	19	4.7776			35.2	2.1200
2	4.8468	2.0132	20	4.7818			36	2.0883
3	4.8423	2.0204	21	4.7872			37	2.0550
4	4.8362	2.0307	22	4.7940			38	2.0274
5	4.8293	2.0442	23	4.8021			39	2.0047
6	4.8219	2.0610	24	4.8116			40	1.9863
7	4.8144	2.0816	25	4.8227			41	1.9718
8	4.8071	2.1066	26	4.8354			42	1.9609
9	4.8001	2.1372	27	4.8500			43	1.9534
10	4.7937	2.1740	28	4.8664			44	1.9487
11	4.7879		28.3	4.8716	4.8522	0.0194	45	1.9467
12	4.7829		29	4.8846	4.8718	0.0128		
13	4.7787		30	4.9049	4.8997	0.0052		
14	4.7756		31	4.9279	4.9271	0.0008		
15	4.7736		31.7	4.9451	4.9451	0		
16	···		32	4.9542				
16.2	4.7727		33	4.9862				
17	4.7728		34					

TABLE III. F_{B1}, F_{B2}, F_C, and F_R (in units of 10^8 G) in the {110} plane. The angle θ is measured from the ⟨001⟩ axis.

θ	F_{B1}	F_R	θ	F_{B1}	F_{B2}	F_C
0	4.8513	2.0074	14	4.7536		
1	4.8511	2.0089	15	4.7460		
2	4.8499	2.0129	16	4.7391		
3	4.8477	2.0198	16.6	4.7352	4.6554	0.0798
4	4.8438	2.0296	17	4.7333	4.6648	0.0685
5	4.8373	2.0431	18	4.7284	4.6843	0.0441
6	4.8289	2.0614	19	4.7245	4.6982	0.0263
7	4.8197	2.0856	20	4.7218	4.7076	0.0142
8	4.8101	2.1181	21	4.7202	4.7140	0.0062
8.2	···	2.1331	22	4.7200	4.7183	0.0017
9	4.8004		23	4.7215	4.7214	0.0001
10	4.7905		24	4.7249	4.7249	0
11	4.7808		25	4.7318		
12	4.7712		25.8	4.7411		
13	4.7621					

TABLE IV. F_{B1} (in units of 10^8 G) in the {110} plane. The angle θ is measured from the ⟨001⟩ axis. The angle $\theta=54.75°$ corresponds to H along the ⟨111⟩ axis.

θ	F_{B1}	θ	F_{B1}
44.6	4.5137	59	4.4286
45	4.5047	60	4.4365
46	4.4846	61	4.4460
47	4.4679	62	4.4571
48	4.4538	63	4.4699
49	4.4422	64	4.4844
50	4.4328	65	4.5006
51	4.4254	66	4.5187
52	4.4200	67	4.5390
53	4.4164	68	4.5612
54	4.4143	69	4.5853
54.75	4.4136	70	4.6116
56	4.4147	71	4.6403
57	4.4177	72	4.6713
58	4.4223	72.5	4.6899

pression for the torque which is normally neglected[7] and which is proportional to

$$\frac{\pi g}{2}\frac{d(m^*/m_0)}{d\theta}\sin\left(\frac{\pi g}{2}\frac{m^*}{m_0}\right).$$

For Au, however, this term leads to a shift in the minimum of less than 10^{-2} degrees. At the present time we have no adequate explanation for the location of the minimum except a value of g which is different from two.

To check for any major anisotropy in the topology of the neck, the [1$\bar{1}$0] suspension sample was tilted 30° from the vertical about the [111] axis. A plot of F_N versus angle in this plane agrees to within 1% with the results in the {110} plane over the range $54.75°\leq\theta\leq81°$. The effective mass on the other hand was 6.5% lower than the mass in the {110} plane at an angle 24.2° from the ⟨111⟩ axis. Correspondingly, we found that the minimum in the amplitude of the neck oscillations occurred at an angle of 25.6±0.2° from the ⟨111⟩ axis compared to 24.85°±0.2° in the {110} plane.

TABLE V. F_D (in units of 10^8 G) in the {110} plane. The angle θ is measured from the ⟨001⟩ axis.

θ	F_D
78	2.0703
79	2.0493
80	2.0304
81	2.0137
82	1.9990
83	1.9863
84	1.9755
85	1.9666
86	1.9595
87	1.9542
88	1.9504
89	1.9479
90	1.9467

[7] I. M. Lifshitz and A. M. Kosevich, Zh. Eksperim. i Teor. Fiz. **29**, 730 (1955) [English transl.: Soviet Phys.—JETP **2**, 636 (1956)].

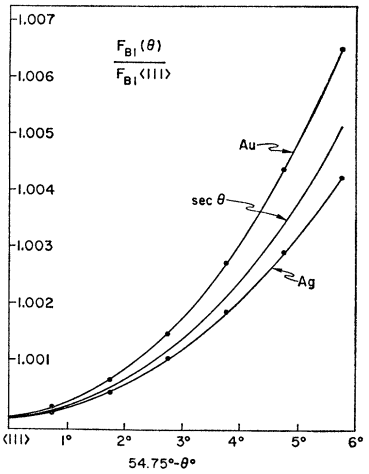

FIG. 5. Plots of the ratios $F_{B1}(\theta)/F_{B1}$ (111) versus angle from the ⟨111⟩ axis for Au and Ag, compared to the variation expected for a cylindrical surface (sec θ).

The angular variation of F_{B1} in Au is qualitatively similar to that observed in Ag. The belly frequency has a minimum near the ⟨100⟩ axis at $\theta\approx22°$ and at $\varphi\approx16°$ (see Figs. 2, 3). In this region we found an additional frequency (F_c) which is zero at $\theta\approx24°$ and at $\varphi\approx31.7°$ and increases very rapidly with decreasing θ and φ. Since the properties of F_c in Au closely resemble those of F_c in Ag, we associate F_c with a difference frequency due to the existence of two types of extremal cross sections around the belly. The frequency associated with the second belly extremal cross section, denoted by F_{B2}, is calculated according to $|F_{B1}-F_{B2}|\equiv F_c$ and is shown plotted in Figs. 2, 3. Although it is clear from the beat waists in the phase that $F_{B1}>F_{B2}$ in the {100} plane, there is no such direct evidence in the {110} plane. We have therefore assumed that $F_{B1}>F_{B2}$, consistent with the interpretation in Ag.

TABLE VI. Effective masses for the neck in the {110} plane and the belly and dog's bone in the {100} plane. All values are within ±3% unless otherwise indicated.

θ	m^*/m_0	φ	m^*/m_0
27.9	0.840	43.6	0.99 } dog's
28.8	0.685	40.5	1.00 } bone
29.0	0.665	28	1.03±0.1 } belly
30.0	0.587	23	1.11±0.1 } belly
30.7	0.530	12	1.08±0.1 } belly
31.5	0.483		
32	0.465		
32.8	0.425		
37.7	0.350		
42.7	0.325		
45.8	0.312		
47.8	0.303		
52.8	0.290		

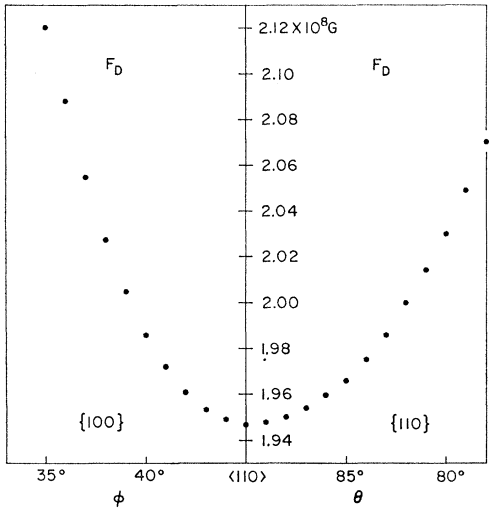

FIG. 6. Plots of the dHvA frequencies of the oscillations associated with the dog's bone in the {100} and {110} planes as functions of φ and θ.

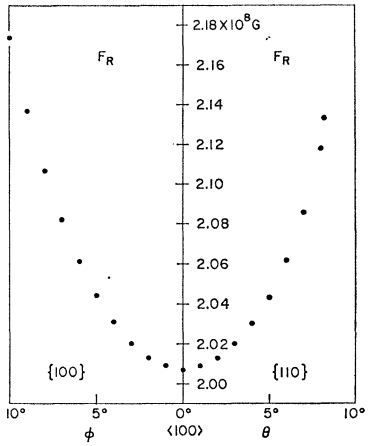

FIG. 7. Plots of the dHvA frequencies of the oscillations associated with the four cornered rosette in the {100} and {110} planes as function of φ and θ.

Near the ⟨111⟩ axis, Au is different from Ag, in that no oscillations were observed that could be associated with a difference frequency. This fact suggests that only one extremal belly cross section exists in this region. In Fig. 5 we show a plot of $F_{B1}(\theta)/F_{B1}(111)$ versus θ for Au and Ag compared to the angular variation of the cross sectional area of a cylinder. It can be seen that F_{B1} for Ag varies more slowly with angle than the corresponding frequency for a cylindrical surface, while F_{B1} for Au varies more rapidly. This suggests that the central belly cross section for the field along the ⟨111⟩ axis is a maximum as a function of k_z (wave vector in the direction of applied field) in Ag and is a minimum in Au, if F_{B1} results from a central orbit. One would therefore not expect Au to have two extremal cross sections in this region.

The frequency variations of the dog's bone and rosette orbits are shown in Figs. 6 and 7, and are similar in behavior to those found in Ag. The limiting angular ranges of the dog's bone in the {100} and {110} planes (calculated with the assumption that the necks have circular cross section), are, respectively, 11.1° and 15.5° compared to the experimentally observed ranges of 9.8° and 12°. For the rosette in the {110} plane, the necks limit the orbits to a calculated angle of 11°, compared to the observed range of 10°.

IV. CONCLUSIONS

The variations of the frequencies of the various de Haas–van Alphen terms have been determined by studying the phases of the oscillations as functions of angle. Relative variations in belly, dog's bone, and rosette frequencies with angle have been measured to better than 5 parts in 10^4 and relative changes in neck frequency have been obtained to within 1 part in 10^3. New low-frequency oscillations have been observed in several regions which can be attributed to multiple extremal cross sections on the belly surface. In contrast to Ag, no low frequency oscillations were observed with the field near the ⟨111⟩ axis.

A study of the amplitude of the neck oscillations and the associated effective masses suggests that the g value in Au might be appreciably different from two.

ACKNOWLEDGMENTS

The authors wish to thank J. Savage and R. Guard for growing the Au crystals and D. Swarthout and P. Romo for orienting the samples. We also wish to thank E. Gertner for his invaluable assistance in data acquisition and analysis. We acknowledge several interesting discussions with G. W. Lehman.